Assessment of Precipitation Anomalies in California Using TRMM and MERRA Data

Andrey K. Savtchenko[1], George Huffman[2], Bruce Vollmer[3]

[1] NASA, Goddard Space Flight Center, Code 610.2 , ADNET Systems, Greenbelt Rd, Greenbelt, MD 20771, USA

[2] NASA, Goddard Space Flight Center, Code 612 , Greenbelt Rd, Greenbelt, MD 20771, USA

[3] NASA, Goddard Space Flight Center, Code 610.2, Greenbelt Rd, Greenbelt, MD 20771, USA

Corresponding author address: Andrey Savtchenko, NASA/GSFC, Code 610.2, Greenbelt Rd, Greenbelt, MD 20771, USA. E-mail: andrey.savtchenko@nasa.gov

Abstract

After more than a decade of moderate seasonal deviations from the expected climate, it is easy to forget that California is actually prone to instabilities in precipitation patterns that occur on various scales. Using modern satellite and reanalysis data we reassess certain aspects of the precipitation climate in California from the past three decades. California has a well-pronounced rain season that peaks in December-February. However, the 95% confidence interval around the climatological precipitation during these months imply that deviations on the order of 60% of the expected amounts are very likely during the most important period of the rain season. While these positive and negative anomalies alternate almost every year and tend to cancel each other, severe multi-year declines of precipitation in California seem to appear on decadal scales. The 1986-1994 decline of precipitation was similar to the current one that started in 2011, and is apparent in the reanalysis data. In terms of accumulated deficits of precipitation, that episode was no less severe than the current one. While El Niño (the warm phase of the El Niño Southern Oscillation, ENSO) is frequently cited as the natural forcing expected to bring a relief, our assessment is that ENSO has been driving at best only 6% of precipitation variability in California in the past three decades. It means El Niño needs to be stronger and longer, in order to have a higher likelihood of a positive impact, and the current one does not match these criteria. Using fractional risk analysis of precipitation populations during normal and dry periods, we show that the likelihood of losing the most intensive precipitation events drastically increases during the multi-year drying events. Since storms delivering up to 50% of precipitation in California are driven by atmospheric rivers making landfall, thus the importance of their suppression and blockage by persistent ridges of atmospheric pressure in the northeast Pacific.

Introduction

California is perceived as a premier habitation, and, apart from its tech sector, is also a top agriculture state, all attributable to its ideal climate. Dollar figures on the agricultural output from California are placing the state at the top amongst agricultural states, leaving Texas ranked only forth by cash receipts [CDFA, 2012]. With $42.6 billion agricultural output at stake [CDFA, 2012], the attention to the lack of precipitation in California is understandable.

Positive and negative precipitation anomalies here alternate every year, tend to cancel each other in consecutive years, and perhaps result in a perceived harmony in the short-term memories. However, there exist numerous studies using historical records from rain gauges and reconstructed tree ring records (Dettinger et al., 1998; Haston and Michaelsen, 1997) that present evidences of strong intrinsic variability of precipitation, and persistent droughts, in the past decades and centuries in California. Pioneering in their nature, these studies also laid the foundation of the present day understanding of the precipitation climate in California.

Comprehensive studies of droughts and drought indexes are also available. Keyantash and Dracup (2002) put together an exhaustive comparative summary of drought indexes. These are complex entities, encompassing more than just precipitation: they also include variables like soil moisture, evaporation, river runoff, lakes levels, etc. While complex in their computation techniques, the drought indices are easy to understand and use by resource analysts, as well as by the general public. They are an excellent tool to evaluate severity of a drought, and relate past episodes and different locations to a common denominator most suitable for agricultural applications.

By no means do we attempt to make a drought assessment, which is out of scope here, using precipitation deficits. In this study we simplify the sources of data and terms in which we quantify the variability in general, and the deficits in particular, of precipitation in California, so that they can be understood and used by a wider readership.

In this effort, we explore the usability of the most recent satellite and reanalysis data as estimators of the likeliest precipitation amounts. We quantify the nominal precipitation season in California, as well as the range of likeliest deviations, observed in the most recent decades. The numbers we issue can be easily converted into absolute amounts of expected fresh water input, around which realistic expectations and contingencies can be built for the state of California on average. As an example, we show the accumulated precipitation deficit in the two consecutive California rain seasons starting in August 2012. These are the optimistic amounts California needs on average to recover, and ideally gradually, rather than in the form of persistent torrential rains, which would shift the issue from drought to different problems like mudslides and flushing the excess precipitation down the rivers. More realistic estimates, however, should consider that the current decline of precipitation in California actually started in the rain season of 2011-2012.

The impact of ENSO on precipitation in general has been extensively studied (Becker et al., 2009; Dettinger et al., 1998). We reevaluate the impact of ENSO on the precipitation in California using most recent satellite and reanalysis data. With only 6% impact on variability of precipitation in California on average, the chances of El Niño having positive influence increase only if it is stronger and longer.

A substantial source of precipitation is delivered to California by atmospheric rivers (Dettinger et al. 2011). Relatively few storms contribute the bulk of California's precipitation each year, and it is the land falling atmospheric rivers that are normally causing most of the largest of these storms. In a long-term average, atmospheric-river storms contribute 20–50% of the state's precipitation totals. However, they can be weakened or even blocked by large ridges of atmospheric pressure forming in the northeast Pacific. We demonstrate the high probability of losing the most intensive precipitation events during multi-year dry episodes, which implies on the persistency and dominating role of the blocking ridges. This indeed can be clearly seen in the yearly averages of the anomalies of winds and precipitation from MERRA.

Data and methods used

The satellite observations we use are data from the joint NASA and Japan Aerospace Exploration Agency (JAXA) mission, Tropical Rainfall Measuring Mission (TRMM). In particular, we use the version 7 of 3B43, TRMM and Other Data Precipitation Product (Huffman, 2007) which is aggregated to monthly intervals. The latter product is output from TRMM Multi-Satellite Precipitation Analysis (TMPA; computed at monthly intervals), which combines the estimates generated by the TRMM and several other satellites. Furthermore, Version 7 of this product shifted to using the rain gauge analysis from the Global Precipitation Climatology Center (GPCC) throughout, rather than employing the one from the Climate Analysis and Monitoring System (CAMS). The 3B43 observations of rainfall are at 1/4x1/4 degree grid boxes for each month. They are available from January 1998, till October 2014.

The reanalysis data are from the Modern-Era Retrospective Analysis for Research and Application (MERRA). MERRA data are derived from the Goddard Earth Observing System version 5 (GEOS-5) data assimilation system. It is a combination of a NASA general circulation model (Rieneker et al., 2007), and the grid point statistical interpolation analysis developed in collaboration with the National Centers for Environmental Prediction. We use the monthly time-averaged surface fluxes diagnostics (short name MATMNXFLX) for the total surface precipitation flux, and the monthly assimilated state (short name MAIMCPASM) for the winds. The surface diagnostic is produced on a 2/3x1/2 (longitude x latitude) degree grid, while the assimilated state is given at 1.25x1.25 deg. There are numerous references describing in details the MERRA data and the underlying incremental analysis update assimilation system (Bloom et al., 1996; Bosilovich et al., 2011). The MERRA data are available from January 1979, until present.

For definiteness, we use standard shape files to extract data over California only. Where appropriate, Student's t-test of 95% confidence level is applied, and thus only the results that are statistically significant at 95% confidence level are presented. For example for anomalies, the hypothesis is that the local monthly precipitation does not deviate from the multi-decadal climatology for that month. Only when this hypothesis is rejected at 95% confidence, the deviations are used as confident anomalies. Paraphrased, we show only the anomalies that deviate with high degree of confidence from the naturally occurring variability in the past decades (35 years for MERRA, and 17 years for TRMM). Thus it should be understood that every time we use words "confident" and "confidently", test of significance was applied.

As an ENSO indicator we use the Multivariate ENSO Index (MEI) provided by Wolter and Timlin (1993; 1998).

Our risk analysis of losing high intensity precipitation events is an approach very similar to what is known as fraction of attributable risk. The latter is frequently applied in studies of increased frequency (risk) of certain anomalies, (Knutson et al., 2014). In our case, it is calculated as a difference between frequencies of occurrence of the most intensive precipitation in the exposed and normal populations, relative to the frequency of occurrence in the normal population: R=(Fe-Fn)/Fn. For the sake of simplicity, the exposed population is drawn from the precipitation series during the decline of precipitation, whereas the rest are considered normal population. The threshold value for the most intensive precipitation is set to that of the 95 percentile of the monthly precipitation anomalies (deviations from the average climate) in the normal population. Similarly, the risk analysis is applied to the weakest 5 percentile of precipitation. The frequencies of occurrence are normalized such that the sum of all frequencies in a histogram is equal to 1.

Results

MERRA is a result of many years of refining of assimilations techniques. It is based in particular on incremental analysis update, where the difference between general circulation model forecast and optimally fused ground and satellite observations is forcing a second, corrective run of the circulation model, (Bosilovish at al., 2011; Rienecker et al., 2011). The combined satellite retrieval, TMPA (Huffman et al., 2010), similarly is in a state of quality and maturity that allows users in many countries to apply it as a true observation when radar or rain gauge measurements are not available.

Thus, the expected precipitation climate over California in the most recent decades estimates consistently from reanalysis and satellite data, Figure 1, and is in agreement with the California climate reported in the past (Caldwell et al., 2009). If by March-April California does not receive its regular amounts, it will very likely miss the target until the next water season. Even though the seasonal precipitation pattern is well pronounced in Figure 1, strong variability is manifested by the length of the bars in the plot. The bars represent the two-side 95% confidence interval for the climate of the month, as an average of all grid cells in California, from the TRMM data. Similar are the confidence intervals from MERRA, not shown for the sake of clarity. Within the peak of the rain season, December-February, dry or wet anomalies on the order of 1 mm/day, which is about 30% of expected amounts, are very likely to happen in any one year.

The time series of the monthly precipitation anomalies, Figure 2, aid in understanding the large confidence intervals in Figure 1. Confidently large wet and dry anomalies are most common in the rainy season, in the winter. The anomalies estimates from MERRA and TRMM are so consistent, that they appear as overlapping lines for the time period of the TRMM mission. We also note the lack of any artificial trends in the MERRA anomalies of precipitation in California in Figure 2. This is a manifestation that neither the MERRA precipitation climate, nor the anomalies (for California) are impacted by the onset of AMSU data from *NOAA-15* (November 1998) and *NOAA-16* (January 2001) satellites. The impact of AMSU on the MERRA assimilation system has been discussed by Robertson et al. (2011).

While Figure 2 demonstrates the magnitude of precipitation variability in California, it cannot reveal long-term accumulations of deficits and excesses. The combination of the strength and duration of the successive precipitation anomalies accumulates over months and years, resulting in long-term deficits and surpluses.

We demonstrate accumulated anomalies by computing cumulative sum of the time series of the anomalies in Figure 2, and present the result in Figure 3. Now it becomes clear that, as a state-wide average, California received cumulative surpluses during most of the past three decades. There was a sharp accumulation of precipitation that started in 1982, in a recovery to a previous dry period, and that lasted for about five years, until 1986.

Starting in 1986, the climate in California shifted to a pattern of persistent deficits that gradually deepened to levels not seen in the past 35 years (Figure 3). In the winter of 1994-1995 the precipitation started to rebound, with a particularly strong recovery in the winter of the strong 1997-1998 El Niño. The current decline of precipitation, an episode that Figure 3 implies started in 2011, shows up as very similar to the 1986-1994 episode.

For the overlapping period of 1998-2011, TRMM and MERRA compare closely (Figure 3). Both reveal that these 13 years were characterized with mild precipitation-deficit seasons that were alternated and comfortably balanced by precipitation-surplus seasons that were relatively stronger and longer. MERRA and TRMM practically overlap in reflecting the decline of precipitation in the most recent dry episode. We'll turn to this period to assess the rate at which precipitation deficit accumulated, using both MERRA and TRMM.

The climatologically expected accumulations of precipitation from TRMM and MERRA, averaged over California only, are presented in Figure 4. Even though the expected means are computed over 35 years of MERRA, and 17 years of TRMM data, both data sets give very close estimates of expected accumulation of precipitation over a year, Table 1. Both TRMM and MERRA are very consistent in estimating the accumulated 2-year deficit of precipitation at about -330 mm.

Table 1. Expected and received 1-year accumulations, and the resulting 2-year accumulated deficit, (mm)

	TRMM	MERRA
Expected	518	487
2012-2013	382	360
2013-2014	325	284
Deficit	-329	-330

For comparison, in Figure 4 we also plot the accumulated surplus of precipitation in the 2004-2005 water season coincident with moderately strong but prolonged El Niño. TRMM shows a more optimistic estimate of the surplus, Table 2, than MERRA. However, even this more favorable estimate shows that an “above average” El Niño may not help to completely offset declined precipitation similar to the most recent episode, and resolve the deficit in one year. Technically, to eliminate the deficit by the end of the 2014-2015 rain season (that is, August 2015), California should receive the expected for the season and the accumulated deficit, to a total of 847 mm. Our early estimates (not shown), using less accurate real-time TRMM and GEOS-5 forecast, reveal California received about 350 mm, from August 2014 till late March 2015. This means that the state must receive almost yearly amounts for the remaining months of the current rain season, April-July, 2015. Since these are the months when the precipitation is seasonally declining (Figure 1), the chances of full recovery in this season are slim.

Table 2. Expected and received accumulations, and accumulated surplus (all in mm) during 2004-2005 El Nino

	TRMM	MERRA
Expected	518	487
2004-2005	745	645
Surplus	+227	+158

The two onsets of substantial recoveries from precipitation deficits, in 1982 and in 1998(Figure 3) coincide with the two strongest El Niños on the record for the duration of MERRA data. The coincidence of the two strongest El Niños with the onset of the two multi-year periods of favorable precipitation, while circumstantial given the short record considered here, should not be completely dismissed. The impact of ENSO on precipitation has been extensively studied (Becker et al., 2009; Dettinger et al., 1998).

In the next section we re-evaluate the portion of California precipitation variability that is driven by ENSO. We built anomalies using 3-month sliding average at every grid cell, and for the climate base period use all data available from MERRA (1979-2014), and TRMM (1998-Sep 2014). Thus built anomalies at every grid cell are then regressed with the ENSO index. The result is actually the Pearson correlation coefficient between precipitation anomalies and ENSO index at every grid cell. The correlation coefficient is tested for 95% confidence, and only the grid cells that pass the test are shown in Figure 5. Precipitation over most of California is confidently influenced by ENSO. The positive correlation means that the precipitation is very likely enhanced during the El Niño, the warm phase of ENSO, and suppressed during the La Nina, the cold phase. We estimate the portion of precipitation variability that is driven by ENSO, by taking the square of the correlation coefficient at every grid cell in Figure 5, and then computing the area average over California only. TRMM and MERRA are again consistent, estimating that only 5-6% of precipitation variability in California is driven by ENSO, Table 3. This leaves lots of chances for El Niño, and in particular the weak events, to have no favorable effect on the precipitation in California.

Table 3. Precipitation variability in California contributed by ENSO, in percents

	TRMM	MERRA
contribution (%)	6	5

We now assess the risks of receiving anomalously weak precipitation, and risks of losing intensive precipitation events, during the extensive periods of declined precipitation over California, in the MERRA and TRMM record. Let's call the subset time series of these precipitation anomalies "exposed population". The risks are expressed in terms of increased frequency of anomalously weak precipitation, and decreased frequency of intense precipitation, during periods of declining precipitation (exposed population), all relative to “normal” periods (normal population). Taking advantage from the longer MERRA record, we define as normal population the MERRA subset from 1/1979 to 6/1986, and from 8/1994 to 6/2011. Whereas the two abnormal periods with declining precipitation are defined as from 7/1986 to 7/1994, and from 7/2011 to 7/2014. We will regard the two periods of declining precipitation separately to assess their relative severity. Also, we will validate the risks of anomalous precipitation for the most recent dry period estimated from both, MERRA and TRMM data. The TRMM normal precipitation population is from 1/1998 to 6/2011, and the period of declined precipitation is the same as the second one for MERRA, from 7/2011 to 7/2014.

The histograms of monthly precipitation anomalies over California only are shown in Figure 6. The dramatic decline of the frequency of intense precipitation events (positive anomalies) revealed by TRMM for the recent dry period stands out immediately. This loss is apparent in MERRA histograms as well, even though to a lesser extent. Both TRMM and MERRA histograms manifest increase in the frequency of occurrence of anomalously weak precipitation (or longer periods of no precipitation) during the dry periods. MERRA implies that this process was even more severe in the 1986-1994 dry episode.

The normalized frequencies Fe, Fn in the risk analysis R=(Fe-Fn)/Fn are computed by integrating the histograms from Figure 6. The threshold values used in the integration are the 5 and 95 percentile of precipitation anomalies in the normal population. The threshold values are shown as vertical dotted lines in Figure 6. The frequencies Fe are computed from the histograms of the exposed populations, while Fn are computed from the histograms of the normal populations.

TRMM and MERRA yield somewhat different estimates of risks in their overlapping period of 2011-2014, Table 4. TRMM data indicate that the risk of losing high intensity precipitation dominated, whereas MERRA implies that the risk of more frequent weak precipitation doubled, during this period of declining precipitation. This is perhaps normal to expect, given the coarser MERRA grid resolution that should smooth the most intensive precipitation, but would otherwise come up even on average when closing global mass and energy budgets (Bosilovich et al., 2011). Indeed on area-average scale, precipitation anomalies from TRMM and MERRA are shown here to be in excellent agreement, Figures 2-3. Taking MERRA only, the current decline of precipitation is characterized by higher risk of disappearing of intensive precipitation, which is replaced by much likelier weak precipitation.

Table 4. Risks of anomalous deviations, using TRMM and MERRA data, (%)

	MERRA		TRMM
	1986-1994	2011-2014	2011-2014
Loss of intense precipitation	55	63	87
Gain of weak precipitation	62	100	61

The increased risk of disappearance of intense precipitation reflects the suppression of atmospheric rivers that are normally causing most of the largest of these storms (Dettinger et al. 2011). The driving force behind that is the persistent ridge of high atmospheric pressure in the northeast Pacific Ocean. The strength of the resulting anomalous geopotential heights, as well as their attribution to anthropogenic forcing, has been analyzed in detail (Herring et al., 2014). Figure 7 demonstrates that MERRA very clearly reflects this anomaly. Instead of geopotential heights, though, we show the vector field of wind anomalies at 850 mb, averaged over the entire 2013. The MERRA precipitation anomalies for the same time period are overplotted as shades. Since this is an yearly average, apparently the winds anomalies respond with very persistent anticyclonic pattern in the northeast Pacific. The wind anomalies are easterly at the south edge of the vortex, i.e. working against the atmospheric rivers. Precipitation anomalies are collocated, extending as a dry river from the north California into the east Pacific.

Summary

The satellite observations and reanalysis considered here, TRMM and MERRA, are very consistent in depicting the precipitation climate in California. Both estimate properly the well-pronounced water season peaking in December-February. However, these data also reveal the inherently unstable character of precipitation in California. Normally, when precipitation is not in a multi-year declining regime, dry and wet deviations on the order of 30% of the expected climate are very likely in any one year.

Another decline of precipitation, similar to the one persisting now, occurred in California in 1986-1994. A number of research groups conclude that the frequency of the blocking atmospheric patterns driving these episodes has increased since the preindustrial age (Herring et al., 2014). Anthropogenic attributions left aside, every next dry episode is still very likely to be felt stronger. Assuming perfect climate, precipitation amounts in California are finite and constrained at about 500 mm/m^2 per year. Whereas the population and land use are growing, and thus are likely to exert more significant stresses on water resources demands than climate warming (Hanak and Lund, 2008).

TRMM and MERRA are in agreement that ENSO is driving on average only about 6% of precipitation variability in California, and, although not strong, this correlation is confidently positive. Thus, stronger El Niños (the warm phase of ENSO), developing before the peak of the precipitation season, like the ones in the winters of 1982-1983 and 1997-1998, are very likely to force more precipitation. That strong El Niños are rare - in the past 35 years, these were the only two of such strength. The current El Niño is weak and most likely will not facilitate any relief in the 2014-2015 water season.

The episodes of declining precipitation in 1986-1994, and the current one that started in 2011 and is still ongoing, are characterized by high risk of losing the most intensive precipitation. TRMM data, being at finer spatial resolution, assess the risks of losing the most intensive 5% of storms to have been at almost 90% for the 2011 episode. Since MERRA data covers both, we can look at how the two episodes compare. MERRA data implies that the loss of the most intensive 5% of storms have been more likely in the current episode. The dramatic difference in the current episode is the doubled likelihood of very weak precipitation (the weakest 5%) as compared to normal periods. In these terms, the current episode, from 2011 till currently at February 2015, is more severe than the 1986-1994 decline of precipitation.

The majority of intensive storms that reach California are driven by atmospheric rivers, and hence the observed increased risk of losing these storms implies suppression and blocking of the atmospheric rivers. As an example of the persistency and the scale of the blocking atmospheric pressure patterns, we show the 2013 yearly anomalies of MERRA 850 mb winds and precipitation. The yearly average reveals anticyclonic wind anomalies, resulting from anomalously high atmospheric pressure ridge, dominating the northeast Pacific. The precipitation anomalies are confidently aligned with the anticyclonic vortex and are extending west from California into the Pacific, to where atmospheric rivers would normally arrive from.

Acknowledgements

The TRMM Multi-Satellite Precipitation Analysis (TMPA) are provided by the NASA/Goddard Space Flight Center's Mesoscale Atmospheric Processes Laboratory and the Precipitation Processing System (PPS) at NASA GSFC, which develop and compute the TMPA as a contribution to TRMM. The data are acquired through the Goddard Earth Sciences Data and Information Services Center (GES DISC).

MERRA data used in this presentation have been provided by the Global Modeling and Assimilation Office (GMAO) at NASA Goddard Space Flight Center through the NASA GES DISC online archive.

References

Becker, E. J., E. H. Berbery, and R. W. Higgins, 2009: Understanding the Characteristics of Daily Precipitation over the United States Using the North American Regional Reanalysis. *J. Climate*, **22**, 6268–6286, doi:10.1175/2009JCLI2838.1

Bloom, S.C., L.L Takacs, A. M. Da Silva, and D. Ledvina, 1996: Data Assimilation Using Incremental Analysis Update, *Mon. Wea. Rev.*, **124**, 1256 - 1271

Bosilovich, M., F. Robertson, J. Chen, 2011: Global Energy and Water Budgets in MERRA, *J. of Climate*, **24**, 5721-5739, doi:10.1175/2011JCLI4175.1

Caldwell, P., H. S. Chin, D. Bader, G. Bala, 2009: Evaluation of a WRF dynamical downscaling simulation over California, *Climatic Change*, **95**, 499-521

CDFA – California Department of Food and Agriculture, California Agricultural Production Statistics, 2012, http://www.cdfa.ca.gov/statistics/.

Dettinger, M., D. Cayan, H. Diaz, D. Meko, 1998: North–South Precipitation Patterns in Western North America on Interannual-to-Decadal Timescales, J. Climate, **11**, 3095-3111

Dettinger M., F. Ralph, T. Das, P. Neiman, D. Cayan, 2011: Atmospheric Rivers, Floods and the Water Resources of California, *Water*, **3**, 445-478; doi:10.3390/w3020445

Hanak E., J. Lund, 2008: Adapting California's Water Management to Climate Change, *Public Policy Institute of California*, http://www.ppic.org/content/pubs/report/R_1108JLR.pdf

Haston, L., J. Michaelsen, 1997: Spatial and Temporal Variability of Southern California Precipitation over the Last 400 yr and Relationships to Atmospheric Circulation Patterns, *J. Climate*, **10**, 1836-1852

Herring, S. C., M. P. Hoerling, T. C. Peterson, and P. A. Stott, Eds., 2014: Explaining Extreme Events of 2013 from a Climate Perspective, *Bull. Amer. Meteor. Soc*, 95 (9), S1-S96

Huffman, G.J., R.F. Adler, D.T. Bolvin, G. Gu, E.J. Nelkin, K.P. Bowman, Y. Hong, E.F. Stocker, D.B. Wolff, 2007: The TRMM Multi-satellite Precipitation Analysis: Quasi-Global, Multi-Year, Combined-Sensor Precipitation Estimates at Fine Scale, *J. Hydrometeor.*, **8**, 38-55

Huffman, G.J., R.F. Adler, D.T. Bolvin, E.J. Nelkin, 2010: The TRMM Multi-satellite Precipitation Analysis (TMPA). Chapter 1 in *Satellite Rainfall Applications for Surface Hydrology*, F. Hossain and M. Gebremichael, Eds. Springer Verlag, ISBN: 978-90-481-2914-0, 3-22.

Knutson, T., F. Zeng, A. Wittenberg, 2014: Seasonal and Annual Mean Precipitation Extremes Occurring During 2013: A U.S. Focused Analysis [in “Explaining Extremes of 2013 from a Climate Perspective”]. *Bull. Amer. Meteor. Soc.*, 95, (9), S19-S23

Keyantash, John, John A. Dracup, 2002: The Quantification of Drought: An Evaluation of Drought Indices. *Bull. Amer. Meteor. Soc.*, **83**, 1167–1180.

Rienecker, M., and Coauthors, 2011: MERRA: NASA's Moddern-Era Retrospective Analysis for Research and Applications. *J. Climate*, **24**, 3624-3648

Robertson, F. R., M. G. Bosilovich, J. Chen and T. L. Miller 2011: The Effect of Satellite Observing System Changes on MERRA Water and Energy Fluxes, *J. Climate*, **24**, 5197-5217

Wolter, K., and M.S. Timlin, 1993: Monitoring ENSO in COADS With a Seasonally Adjusted Principal Component Index. *Proc. of the 17th Climate Diagnostics Workshop, Norman, OK, NOAA/NMC/CAC*, NSSL, Oklahoma Clim. Survey, CIMMS and the School of Meteor., Univ. of Oklahoma, 52-57

Wolter, K., and M. S. Timlin, 1998: Measuring the Strength of ENSO Events - how does 1997/98 rank? *Weather*, **53**, 315-324.

FIGURE CAPTION LIST

Figure 1. Precipitation climate in California, from TRMM observations and MERRA reanalysis. The bars reflect the 95% confidence interval of TRMM climatology.

Figure 2. Precipitation anomaly from MERRA and TRMM. Area average over California only, using 95% confident anomalies.

Figure 3. Cumulative sum of precipitation anomalies from Figure 2.

Figure 4. Accumulation of precipitation in California. Expected average accumulation (climatology) from MERRA and TRMM, as compared to El Nino 2004, and the recent dry seasons of 2012-2013, and 2013-2014.

Figure 5. Monthly precipitation anomalies from TRMM and MERRA regressed on MEI, at 95% confidence. Red colors indicate enhanced precipitation during El Niño (warm phase), and vice versa during La Niña (cold phase).

Figure 6. Histograms of normalized frequencies of monthly precipitation anomalies over California only. Dotted lines indicate the 5 and 95 percentiles threshold values in the histograms of the normal populations.

Figure 7. Anomalies of MERRA winds at 850 hPa (vectors), and precipitation (shades) in 2013.

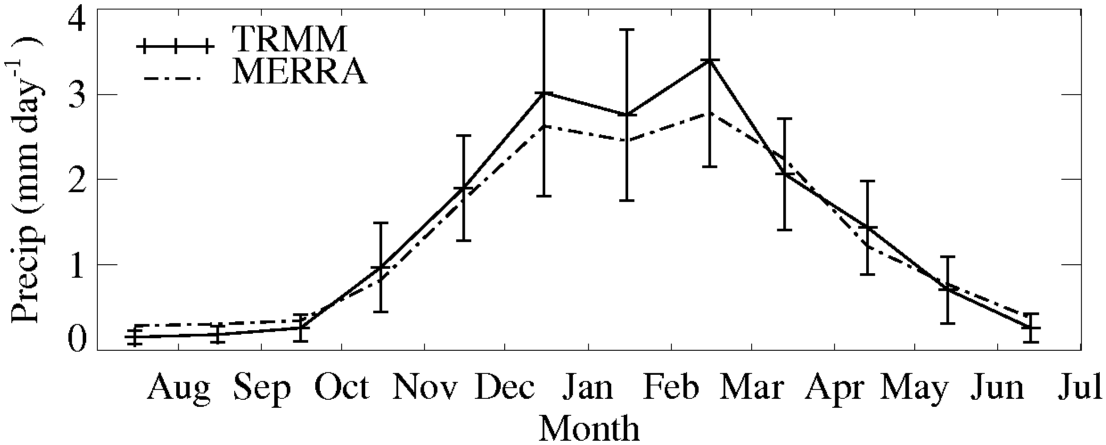

Figure 1. Precipitation climate in California, from TRMM observations and MERRA reanalysis. The bars reflect the 95% confidence interval of TRMM climatology.

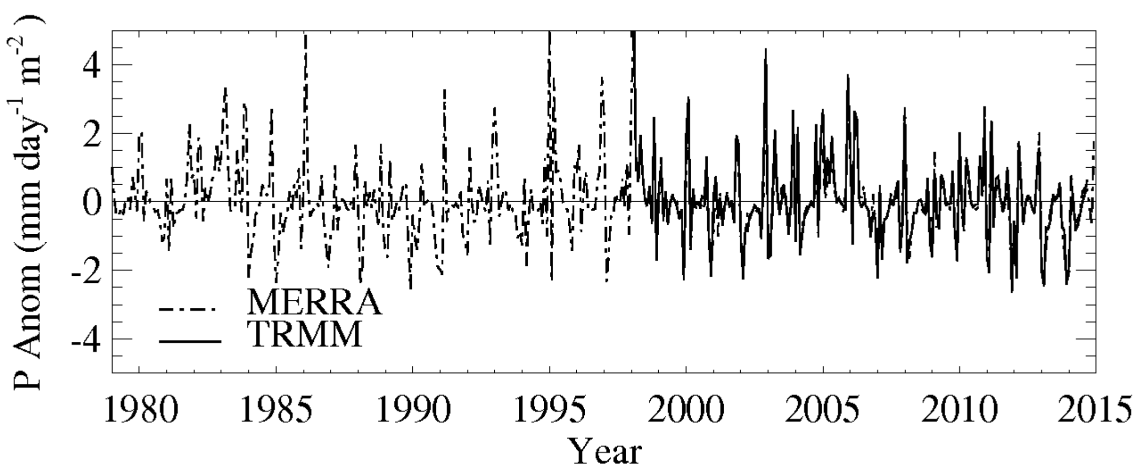

Figure 2. Precipitation anomaly from MERRA and TRMM. Area average over California only, using 95% confident anomalies.

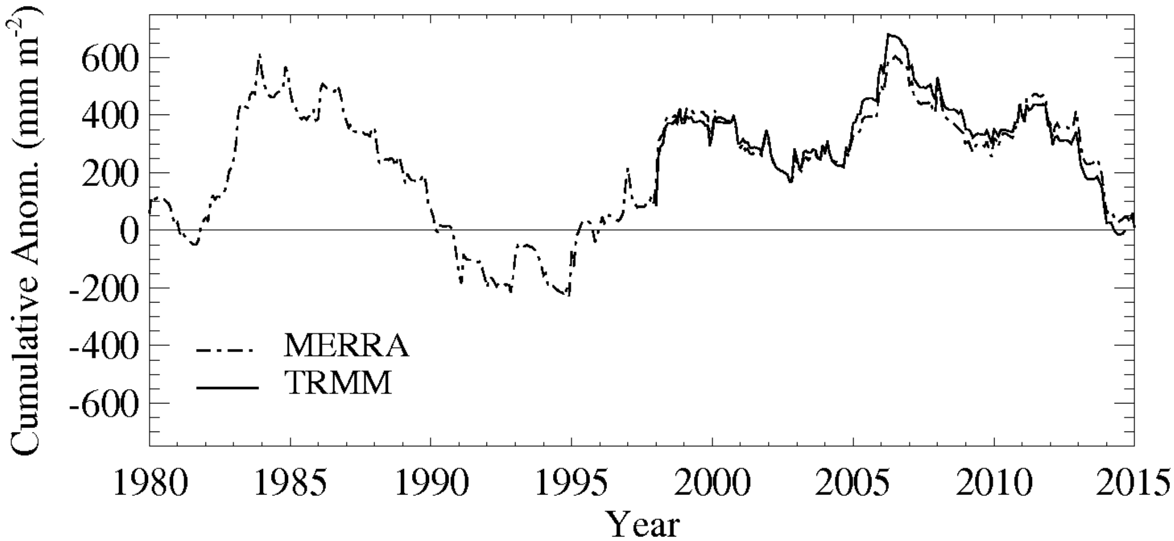

Figure 3. Cumulative sum of precipitation anomalies from Figure 2.

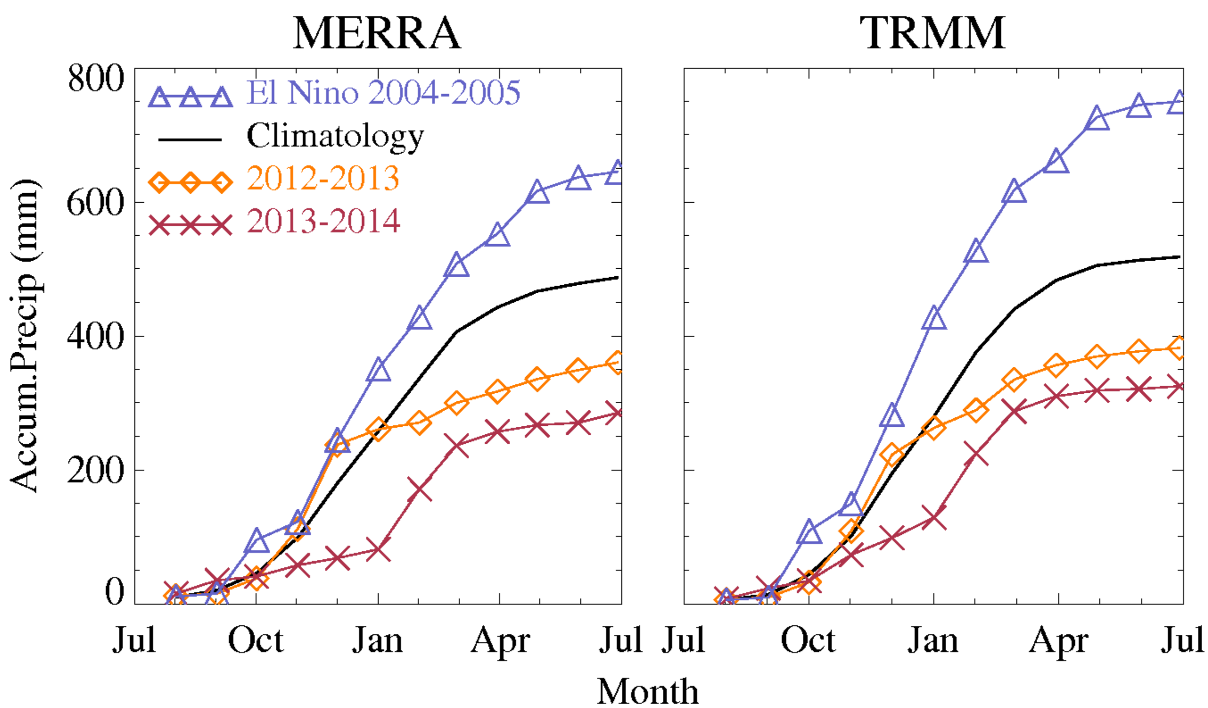

Figure 4. Accumulation of precipitation in California. Expected average accumulation (climatology) from MERRA and TRMM, as compared to El Nino 2004, and the recent dry seasons of 2012-2013, and 2013-2014.

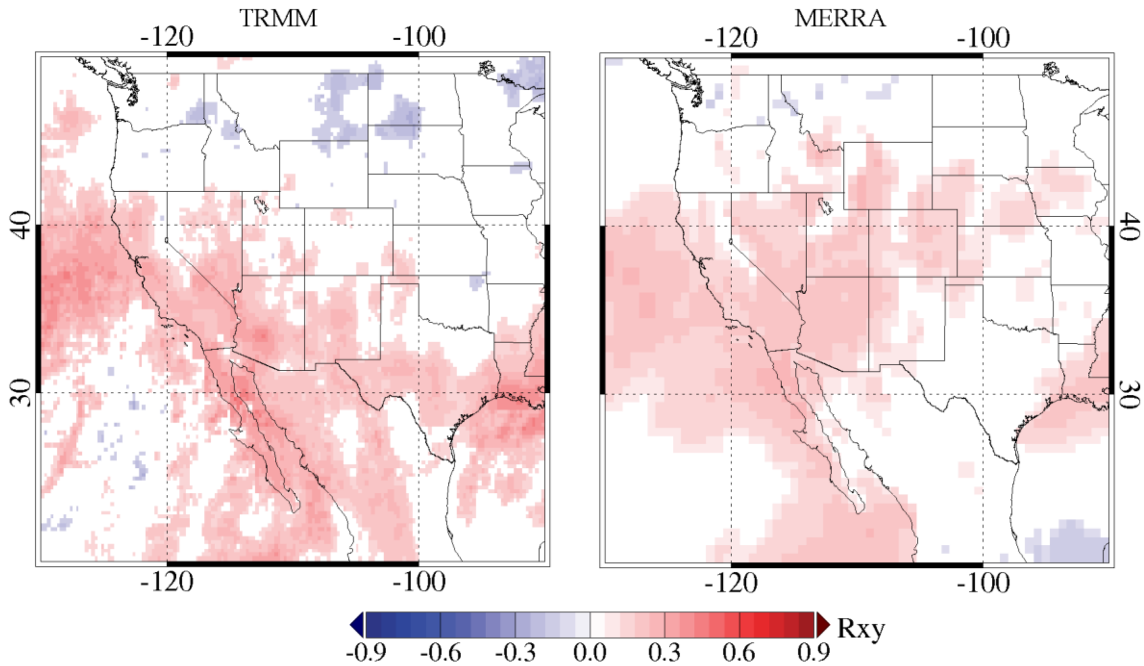

Figure 5. Monthly precipitation anomalies from TRMM and MERRA regressed on MEI, at 95% confidence. Red colors indicate enhanced precipitation during El Niño (warm phase), and vice versa during La Niña (cold phase).

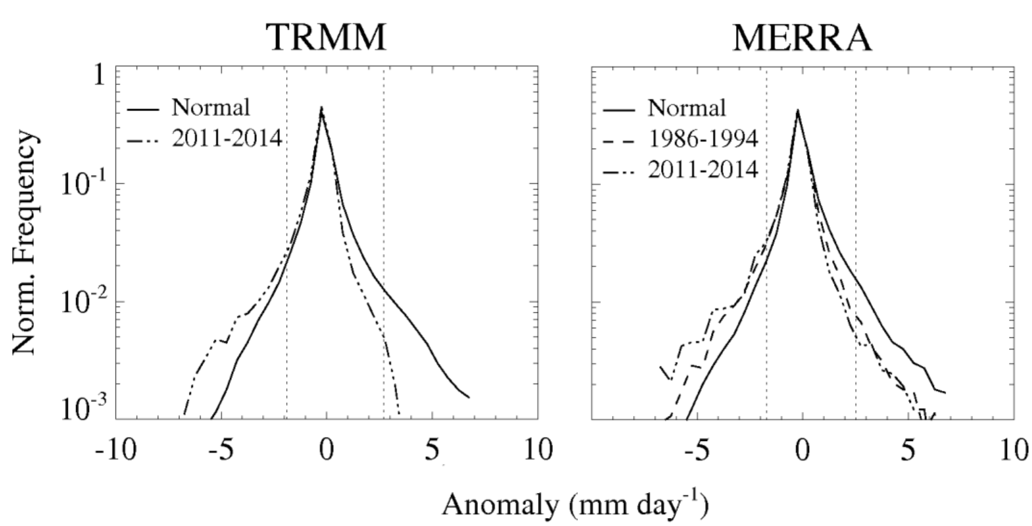

Figure 6. Histograms of normalized frequencies of monthly precipitation anomalies over California only. Dotted lines indicate the 5 and 95 percentiles threshold values in the histograms of the normal populations.

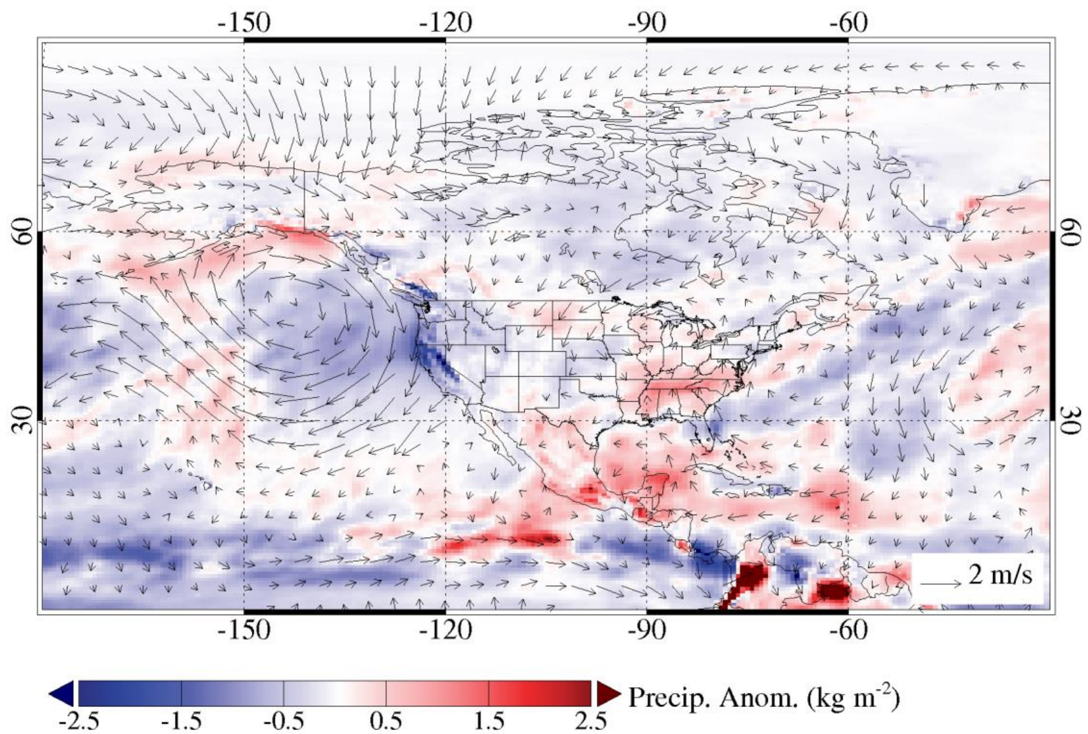

Figure 7. Anomalies of MERRA winds at 850 hPa (vectors), and precipitation (shades) in 2013.